8-2014

Realization of Negative Index in Second-order Dispersive Metamaterials Using Standard Dispersion Models for Electromagnetic Parameters

Tarig A. Algadey
University of Dayton

Monish Ranjan Chatterjee
University of Dayton, mchatterjee1@udayton.edu

Realization of negative index in second-order dispersive metamaterials using standard dispersion models for electromagnetic parameters

Tarig A. Algadey1[a] and Monish R. Chatterjee2[b]

[a]University of Dayton, Dept. of ECE, 300 College Park, Dayton, OH 45469-0232;

ABSTRACT

In recent work, electromagnetic propagation velocities for plane waves in dispersive metamaterials were calculated assuming frequency dispersion up to the second order. The three velocities were expressed in terms of dispersive coefficients under certain simplifying constraints. Frequency domains were found to exist around resonances where group and phase velocities are in opposition, implying possible negative index behavior. In this paper, we incorporate in the derived equations physical models (including Debye, Lorentz and Condon) for material dispersion in permittivity, permeability and chirality in order to further examine the consequences of second-order dispersion leading to negative index for practical cases, and also evaluate the resulting phase and group indices.

Keywords: Group and phase velocities, chiral constitutive relations, second-order dispersive, counter-propagation, Dispersive coefficients.

1. INTRODUCTION

Electromagnetic velocities offer a convenient route to predicting optical refraction in a material as a function of frequency and specific material parameters. Thus, it is known that in domains where the (real parts of) permittivity and permeability of the medium are positive, the resulting phase index is also positive. Conversely, if both these parameters have negative real parts, the material begins to exhibit negative index characteristics. Negative index may be shown to occur when the group and phase velocities in the material become counter-propagating. To examine whether and when this might happen, a spectral approach involving slowly time-varying phasors and chiral constitutive relations was recently developed, and the velocities for dispersive permittivity, permeability and chirality were derived up to first and second order.[1–3] For both cases, it is found that the presence of chirality automatically makes a propagating plane wave devolve into circular polarizations. Additionally, it is found that the energy velocity is not generally expressible independent of field amplitude for second-order dispersion, unless specific assumptions are made regarding dispersive coefficients for the three parameters of interest. However, phase and group velocities may still be expressed in terms of coefficients only (independent of field amplitude) even for second-order. In this paper, we incorporate in the derived equations physical models (including Debye, Lorentz and Condon) for material dispersion in permittivity, permeability and chirality in order to further examine the consequences of second-order dispersion leading to negative index for practical cases, and also evaluate the resulting phase and group indices.[4–6] In section 2 we present a quick review of EM field solutions under seond-order material dispersion and associated propagation velocities previously derived by Banerjee and Chatterjee.[1,2] We show that once again the fields exhibit circular polarization when the material parameters expanded up to the second order. We derive normalized expressions for the energy velocity based on the Poynting vector and the stored energy density inside the medium. Initially, we find that the ratio of these two quantities can no longer be made independent of the (unknown) field component $\tilde{E}_{px}$.[1] As a result, this limited the ability to calculate $\tilde{v}_{e3N}$ independent of $\tilde{E}_{px}$. Through sheer serendipity, it turned out that choosing a certain balancing of parametric ratios between the different types of dispersion in the material, several of the terms in the original derivation conveniently canceled, thereby leaving a result where the unknown $\tilde{E}_{px}$ terms dropped out,

Further author information: (Send correspondence to Monish R. Chatterjee1.)
Monish R. Chatterjee1.: E-mail: : mchatterjee1@udayton.edu, Telephone: 1 937 229 3594
Tarig A. Algadey.: E-mail: talgadey@gmail.com, Telephone: +1 484 632 0524

Metamaterials: Fundamentals and Applications 2014, edited by Nader Engheta, Mikhail A. Noginov, Nikolay I. Zheludev,
Proc. of SPIE Vol. 9160, 91602I · © 2014 SPIE · CCC code: 0277-786X/14/$18 · doi: 10.1117/12.2065262

leaving a velocity expression similar to the purely parameter-dependent results that were previously obtained in ref. 2. By this a choice we find that the energy velocity can be calculated and normalized independent of field amplitudes. The phase and group velocities ($\tilde{v}_{p3N}$,$\tilde{v}_{g3N}$) normalized are likewise obtained after considerable algebra. In section 3 we track the behavior of chiral material in terms of the phase and group velocities when the material parameters have expanded up to the second order, we assume the lorentzian (Drude) models for relative permittivity and permeability and the Condon dispersive model for chirality.[4] Section 4 concludes this paper with a summary of the derived second-order fields and velocities and their similarities and differences w.r.t. the standard dispersionless and first-order results.

2. PRELIMINARY EXAMINATION OF THE SECOND-ORDER DISPERSIVE MODEL

In this section, we begin by expanding the material parameters up to the second order in frequency using the Taylor series,[1,2] leading to.

$$\begin{pmatrix} \tilde{\varepsilon}_p(\Omega) \\ \tilde{\mu}_p(\Omega) \\ \tilde{\alpha}_p(\Omega) \end{pmatrix} = \begin{pmatrix} \tilde{\varepsilon}_{p0}(\Omega) + (\Omega)\tilde{\varepsilon}'_{p0} + (\Omega^2/2)\tilde{\varepsilon}''_{p0} \\ \tilde{\mu}_{p0}(\Omega) + (\Omega)\tilde{\mu}'_{p0} + (\Omega^2/2)\tilde{\mu}''_{p0} \\ \omega\sqrt{\mu_0\varepsilon_0}(\tilde{\kappa}_{p0} + (\Omega)\tilde{\kappa}'_{p0} + (\Omega^2/2)\tilde{\kappa}''_{p0}) \end{pmatrix}. \tag{1}$$

where $\tilde{\kappa}_p(\Omega)$ is the frequency-dependent chirality parameter, which is dimensionless; $\tilde{\varepsilon}_p(\Omega)$ and $\tilde{\mu}_p(\Omega)$ is called frequency dependent electric permittivity and also is the magnetic permeability. Likewise, the parameter $\tilde{\alpha}_p(\Omega) = \omega\tilde{\kappa}_p\sqrt{\mu_0\varepsilon_0}$, which has the dimension rad m^-1 , is the chiral wavenumber. Since ref 1, we may express the field components to second-order as follows

$$\tilde{E}_{px}(\Omega), \text{arbitrary} \tag{2a}$$

$$\tilde{E}_{py}(\Omega) = j(A_{13} + \Omega B_{13} + \Omega^2 C_{13})\tilde{E}_{px}(\Omega), \tag{2b}$$

$$\tilde{H}_{px}(\Omega) = j(A_{23} + \Omega B_{23} + \Omega^2 C_{23})\tilde{E}_{px}(\Omega), \tag{2c}$$

$$\tilde{H}_{py}(\Omega) = j(A_{33} + \Omega B_{33} + \Omega^2 C_{33})\tilde{E}_{px}(\Omega). \tag{2d}$$

As mentioned, using the above and after considerable algebra (the details may be found in ref 1), the coefficients are found to be:

$$A_{13} = 1, B_{13} = 0, C_{13} = 0. \tag{3}$$

Substituting the above in Eq. (2b) immediately indicates that once again $\tilde{E}_{py} = j\tilde{E}_{px}$. This result implies that even under second-order dispersion, the EM field in the presence of chirality again exhibits circular polarization, as was seen in the first-order case. Thus, the presence of the chiral constitutive relations in the EM analysis automatically leads to circular polarization, independent of dispersion. The resulting Y-component of the electric field leads the X-component by 90^0.

Since ref 1, we have gotten that

$A_{23} = -\sqrt{\frac{\tilde{\varepsilon}_{p0}}{\tilde{\mu}_{p0}}}$, $\quad B_{23} = -\sqrt{\frac{\tilde{\varepsilon}_{p0}}{\tilde{\mu}_{p0}}}(\frac{\tilde{\varepsilon}'_{po}}{2\tilde{\varepsilon}_{p0}} - \frac{\tilde{\mu}'_{po}}{2\tilde{\mu}_{p0}})$, and

$$C_{23} = -\sqrt{\frac{\tilde{\varepsilon}_{p0}}{\tilde{\mu}_{p0}}}(\frac{1}{4}\frac{\tilde{\varepsilon}''_{po}}{\tilde{\varepsilon}_{p0}} - \frac{1}{8}\frac{\tilde{\varepsilon}'^2_{po}}{\tilde{\varepsilon}^2_{p0}} - \frac{\tilde{\mu}'_{po}}{2\tilde{\mu}_{p0}}\frac{\tilde{\varepsilon}'_{po}}{2\tilde{\varepsilon}_{p0}} - \frac{1}{4}\frac{\tilde{\mu}''_{po}}{\tilde{\mu}_{p0}} + \frac{3}{8}\frac{\tilde{\mu}'^2_{po}}{\tilde{\mu}^2_{p0}}). \tag{4}$$

Similarly,

$A_{33} = -A_{23} = \sqrt{\frac{\tilde{\varepsilon}_{p0}}{\tilde{\mu}_{p0}}}$, $\quad B_{33} = -B_{23} = \sqrt{\frac{\tilde{\varepsilon}_{p0}}{\tilde{\mu}_{p0}}}(\frac{\tilde{\varepsilon}'_{po}}{2\tilde{\varepsilon}_{p0}} - \frac{\tilde{\mu}'_{po}}{2\tilde{\mu}_{p0}})$, and

$$C_{33} = -C_{23} = \sqrt{\frac{\tilde{\varepsilon}_{p0}}{\tilde{\mu}_{p0}}}(\frac{1}{4}\frac{\tilde{\varepsilon}''_{po}}{\tilde{\varepsilon}_{p0}} - \frac{1}{8}\frac{\tilde{\varepsilon}'^2_{po}}{\tilde{\varepsilon}^2_{p0}} - \frac{\tilde{\mu}'_{po}}{2\tilde{\mu}_{p0}}\frac{\tilde{\varepsilon}'_{po}}{2\tilde{\varepsilon}_{p0}} - \frac{1}{4}\frac{\tilde{\mu}''_{po}}{\tilde{\mu}_{p0}} + \frac{3}{8}\frac{\tilde{\mu}'^2_{po}}{\tilde{\mu}^2_{p0}}) \tag{5}$$

We next calculate the energy velocity normalized by divide the average Poynting vector by the total stored energy and assuming the material parameter ratios to be given by

$$\frac{\tilde{\varepsilon}'_{po}}{\tilde{\varepsilon}_{p0}} = \frac{\tilde{\mu}'_{po}}{\tilde{\mu}_{p0}}, \tag{6}$$

and

$$\frac{\tilde{\varepsilon}''_{po}}{\tilde{\varepsilon}_{p0}} = \frac{\tilde{\mu}''_{po}}{\tilde{\mu}_{p0}}. \tag{7}$$

indicating balance between first- and second-order dispersions, respectively, between permittivity and permeability.

As mentioned, the assumption above helps us to solve the energy velocity and make it simpler. By using the material parameters in relations (4) and (7), this leads to:

$$A_{23} = -\sqrt{\frac{\tilde{\varepsilon}_{p0}}{\tilde{\mu}_{p0}}},\ B_{23} = -\sqrt{\frac{\tilde{\varepsilon}_{p0}}{\tilde{\mu}_{p0}}}(\frac{\tilde{\varepsilon}'_{po}}{2\tilde{\varepsilon}_{p0}} - \frac{\tilde{\mu}'_{po}}{2\tilde{\mu}_{p0}}) = 0,$$

and,

$$C_{23} = -\sqrt{\frac{\tilde{\varepsilon}_{p0}}{\tilde{\mu}_{p0}}}(\frac{1}{4}\frac{\tilde{\varepsilon}''_{po}}{\tilde{\varepsilon}_{p0}} - \frac{1}{8}\frac{\tilde{\varepsilon}'^{2}_{po}}{\tilde{\varepsilon}^{2}_{p0}} - \frac{\tilde{\mu}'_{po}}{2\tilde{\mu}_{p0}}\frac{\tilde{\varepsilon}'_{po}}{2\tilde{\varepsilon}_{p0}} - \frac{1}{4}\frac{\tilde{\mu}''_{po}}{\tilde{\mu}_{p0}} + \frac{3}{8}\frac{\tilde{\mu}'^{2}_{po}}{\tilde{\mu}^{2}_{p0}}) = 0. \tag{8}$$

As mentioned in ref 1 and using Eqs. (6) and (7), the energy velocity normalized given by

$$\tilde{v}_{e3N}(\Omega) = \frac{-1}{2(\sqrt{\mu_r\varepsilon_r} - \tilde{\kappa}_{p0}) + \Omega^2(\frac{\tilde{\varepsilon}''_{po}\sqrt{\mu_r\varepsilon_r}}{\tilde{\varepsilon}_{p0}} - \tilde{\kappa}''_{p0})}, \tag{9}$$

and assume $\tilde{\mu}_r = \tilde{\varepsilon}_r = 4$, $\tilde{\kappa}_{po} = 5$ and $\tilde{\varepsilon}_{p0} = \varepsilon_r\varepsilon_0$, and $\tilde{\kappa}'_{p0} = \dfrac{\tilde{\varepsilon}'_{po}}{\varepsilon_0}$. This leads to

$$\tilde{v}_{e3N}(\Omega) = \left[\frac{-1}{(-b + \Omega^2 a)}\right], \tag{10}$$

where $b = 2$, $a = (\dfrac{\tilde{\varepsilon}''_{po}}{\varepsilon_0} - \tilde{\kappa}''_{p0})$.

Using the relation $\tilde{v}_p(\Omega) = 1/(K_z/\omega)$, and Eq. (6), we may calculate the phase velocity normalized by using $\tilde{k}_{z3}$ and retaining up to the second order in Ω, as described below.

$$\tilde{v}_{p3N}(\Omega) = \frac{1}{\left(\begin{array}{l} -1 + \Omega[(\frac{\tilde{\varepsilon}'_{po}}{\varepsilon_0}) - \tilde{\kappa}'_{p0}] + \\ \Omega^2[-\frac{1}{2}\tilde{\kappa}''_{p0} + \frac{\tilde{\varepsilon}''_{po}}{2\varepsilon_0}] \end{array}\right)}, \tag{11a}$$

$$\tilde{v}_{p3N}(\Omega) = \frac{1}{C + B\Omega + A\Omega^2}, \tag{11b}$$

$$\tilde{v}_{p3N}(\Omega) = \frac{1}{-1 + (\Omega^2/\Omega_r^2)}, \tag{11c}$$

where $\Omega_r = (-\frac{1}{2}\tilde{\kappa}''_{p0} + \frac{\tilde{\varepsilon}''_{po}}{2\varepsilon_0})^{-1/2}$,and $\tilde{k}_{z3} = -\omega\tilde{\kappa}_p\sqrt{\mu_0\varepsilon_0} + \omega\sqrt{\tilde{\mu}_p\tilde{\varepsilon}_p}$.

Since ref 1, the group velocity normalized determined to be as below:

$$\tilde{v}_{g3N}(\Omega) = \frac{1}{[a + b\Omega + c\Omega^2]}, \tag{12}$$

where, $a = -1,\ \ b = -2\tilde{\kappa}'_{p0} - \omega_0\tilde{\kappa}''_{p0} + \omega_0\frac{\tilde{\varepsilon}''_{p0}}{\varepsilon_0} + 2\frac{\tilde{\varepsilon}'_{p0}}{\varepsilon_0},\ \ c = -\frac{3}{2}\tilde{\kappa}''_{p0} + \frac{3}{2}\frac{\tilde{\varepsilon}''_{p0}}{\varepsilon_0}, \omega_0 = 10^{14}$.

Next step we incorporate in the derived equations (phase and group velocities) physical models (including Debye, Lorentz and Condon) for material dispersion in permittivity, permeability and chirality in order to further examine the consequences of second-order dispersion leading to negative index for practical cases, and also evaluate the resulting phase and group indices.

3. APPLICATION OF PRACTICAL DISPERSIVE MODELS TO THE SECOND-ORDER SYSTEM

To study the performance of the chiral dispersive materials in terms of the normalized phase and group velocities derived previously for propagating signals consisting of pulsed or modulated carriers, we take up the Lorentzian dispersive models for relative permittivity and permeability and the Condon model for chirality, as follows.[4]

$$\tilde{\varepsilon}_{pr}(\omega) = 1 + \frac{(\omega_p^2)}{(\omega_c^2 - \omega^2)} \tag{13}$$

$$\tilde{\mu}_{pr}(\omega) = 1 + \frac{(\omega_m^2)}{(\omega_c^2 - \omega^2)} \tag{14}$$

$$\tilde{\kappa}_{pr}(\omega) = \alpha_c\frac{(\omega)}{(\omega_c^2 - \omega^2)} \tag{15}$$

where $\tilde{\varepsilon}_{pr}(\omega)$,$\tilde{\mu}_{pr}(\omega)$, and $\tilde{\kappa}_{pr}(\omega)$ are respectively the relative (spectral) permittivity, permeability, and chirality admittance of the material under consideration. The frequencies ω_p and ω_m arise from electric polarization and magnetization, respectively, while ω_c represents a (single) resonance in the neighborhood of the applied signal. Also α_c represents a chiral frequency parameter. From Eq. (1), we have the relativity permittivity under second-order material dispersion as follows:

$$\tilde{\varepsilon}_p(\Omega) = \tilde{\varepsilon}_{p0}(\Omega) + (\Omega)\tilde{\varepsilon}'_{p0} + (\Omega^2/2)\tilde{\varepsilon}''_{p0}, \tag{16}$$

where the sideband frequency Ω is equal to $\Omega = \omega - \omega_0$, and ω_0 is the carrier frequency. We may note that typically $\Omega << \omega_0$, and therefore while the carrier may be in the optical domain, the sideband may well be in the RF (thus in the MHz-GHz range).

In case of $\Omega << \omega_c$ the relative spectral permittivity in Eq. (13) can be written as follows:

$$\tilde{\varepsilon}_{pr}(\omega) = 1 + \frac{\frac{\omega_p^2}{\omega_c^2}}{(1 - \frac{\omega^2}{\omega_c^2})}. \tag{17}$$

Using Taylor expansion up to the second-order for the equation above and assuming $\Omega << \omega_c$ and $\omega_0 << \omega_c$, and comparing Eq. (13) with Eq. (16), we will have the following:

$$\tilde{\varepsilon}'_{pr0} = \frac{\tilde{\varepsilon}'_{p0}}{\tilde{\varepsilon}_{p0}} = \frac{2\omega_0\omega_p^2}{\omega_c^4}, \tag{18a}$$

$$\tilde{\varepsilon}''_{pr0} = \frac{\tilde{\varepsilon}''_{p0}}{2\tilde{\varepsilon}_{p0}} = \frac{\omega_p^2}{\omega_c^4}, \tag{18b}$$

$$\tilde{\varepsilon}_{pr0} = \frac{\tilde{\varepsilon}''_{p0}}{2\tilde{\varepsilon}_{p0}} = 1 + \frac{\omega_p^2}{\omega_c^2}, \tag{18c}$$

Similarly, from the relative (spectral) permeability relation and comparing with the Lorentzian dispersive model for relative permeability in Eq. (14), we get the following:

$$\frac{\tilde{\mu}_p(\Omega)}{\tilde{\mu}_{p0}(\Omega)} = 1 + \frac{\Omega\tilde{\mu}'_{p0}}{\tilde{\mu}_{p0}} + \frac{(\Omega^2/2)}{\tilde{\mu}_{p0}}\tilde{\mu}''_{p0}, \tag{19}$$

$$\tilde{\mu}'_{pr0} = \frac{\tilde{\mu}'_{p0}}{\tilde{\mu}_{p0}} = \frac{2\omega_0\omega_m^2}{\omega_c^4}, \tag{20a}$$

$$\tilde{\mu}''_{pr0} = \frac{\tilde{\mu}''_{p0}}{2\tilde{\mu}_{p0}} = \frac{\omega_m^2}{\omega_c^4}, \tag{20b}$$

$$\tilde{\mu}_{pr0} = \frac{\tilde{\mu}''_{p0}}{2\tilde{\mu}_{p0}} = 1 + \frac{\omega_m^2}{\omega_c^2}, \tag{20c}$$

Finally, based on the chirality expression up to second-order material dispersion, the chiral coefficients may be derived as follows:

$$\tilde{\kappa}_p(\Omega) = \tilde{\kappa}_{p0} + (\Omega)\tilde{\kappa}'_{p0} + (\Omega^2/2)\tilde{\kappa}''_{p0}. \tag{21}$$

Wherefrom, upon applying the Condon model as in Eq. (13) , we obtain the following:

$$\tilde{\kappa}_{pr0} = \alpha_c\frac{\omega_0}{\omega_c^2}, \tag{22a}$$

$$\tilde{\kappa}'_{pr0} = \frac{\tilde{\kappa}'_{p0}}{\tilde{\kappa}_{p0}} = \alpha_c\frac{1}{\omega_c^2}, \tag{22b}$$

$$\tilde{\kappa}''_{pr0} = \frac{\tilde{\kappa}''_{p0}}{\tilde{\kappa}_{p0}} = 6\alpha_c\frac{\omega_0}{\omega_c^4}. \tag{22c}$$

We next substitute Eqs. (18a)-(18c), (20a)-(20c), and (22a)-(22c) into Eq. (11a) to compute the normalized phase velocity under the Lorentzian dispersive model for relative permittivity and permeability and the Condon model for chirality. After considerable algebra, we obtain the (normalized) phase velocity as in eq. (11b).[1] To plot phase velocity versus the sideband frequency we assume plausible values for ω_p, ω_m and ω_c.[7] Thus, we begin with the phase velocity as above in Eq. (11c)

$$\tilde{v}_{p3N}(\Omega) = \frac{1}{\left(-1 + \Omega^2[-\frac{1}{3}\alpha_c\frac{\omega_0}{\omega_c^4} + \frac{\tilde{\varepsilon}''_{po}}{2\varepsilon_0}] \right)}, \tag{23}$$

so that after substitution

$$\tilde{v}_{p3N}(\Omega) = \frac{1}{a + \Omega^{-1}b}, \tag{24a}$$

the sideband resonance is at:

$$\Omega_r = \sqrt{\frac{-a}{b}}, \tag{24b}$$

$$\Omega_r = \frac{\omega_c^2}{\sqrt{3\omega_p^2 - 3\alpha_c\omega_0}}. \tag{24c}$$

The phase velocity resonates at approximately 0.998×10^{10} rad/sec. From the plot we note that in this instance, $(\tilde{v}_{p3N})$ transitions from negative to positive.

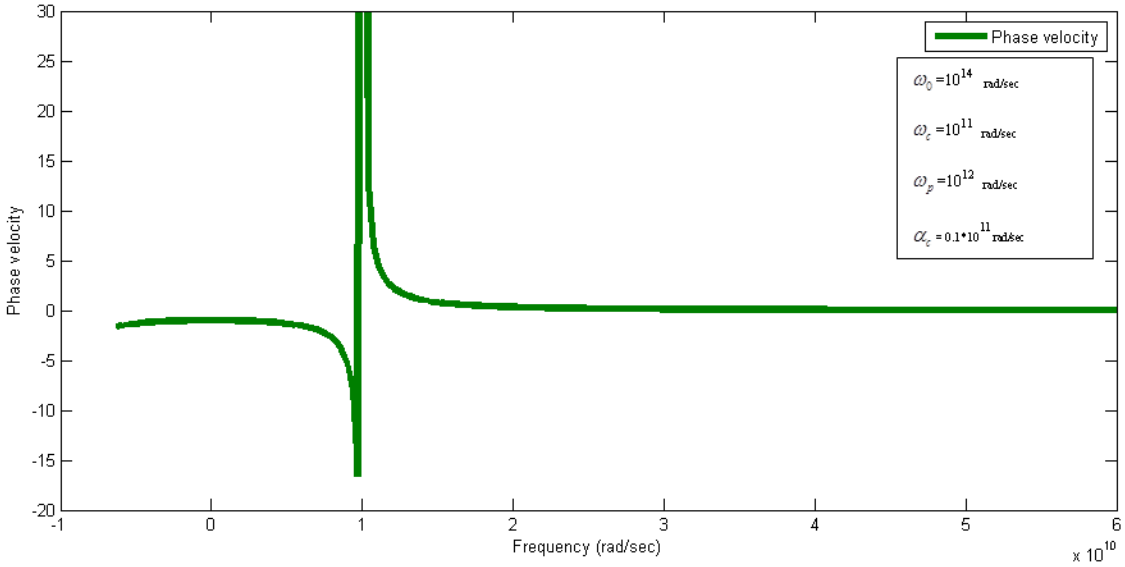

Figure 1. The phase velocity.

Similarly, for the group velocity normalized:

$$\tilde{v}_{g3N}(\Omega) = \frac{1}{[a + b\Omega + c\Omega^2]}, \tag{25}$$

where, $a = -1$, $b = -\omega_0 30\alpha_c \frac{\omega_0}{\omega_c^4} + 8\omega_0 \frac{\omega_p^2}{\omega_c^4}$, $c = -\frac{90}{2}\alpha_c \frac{\omega_0}{\omega_c^4} + \frac{24}{2}\frac{\omega_p^2}{\omega_c^4}$.

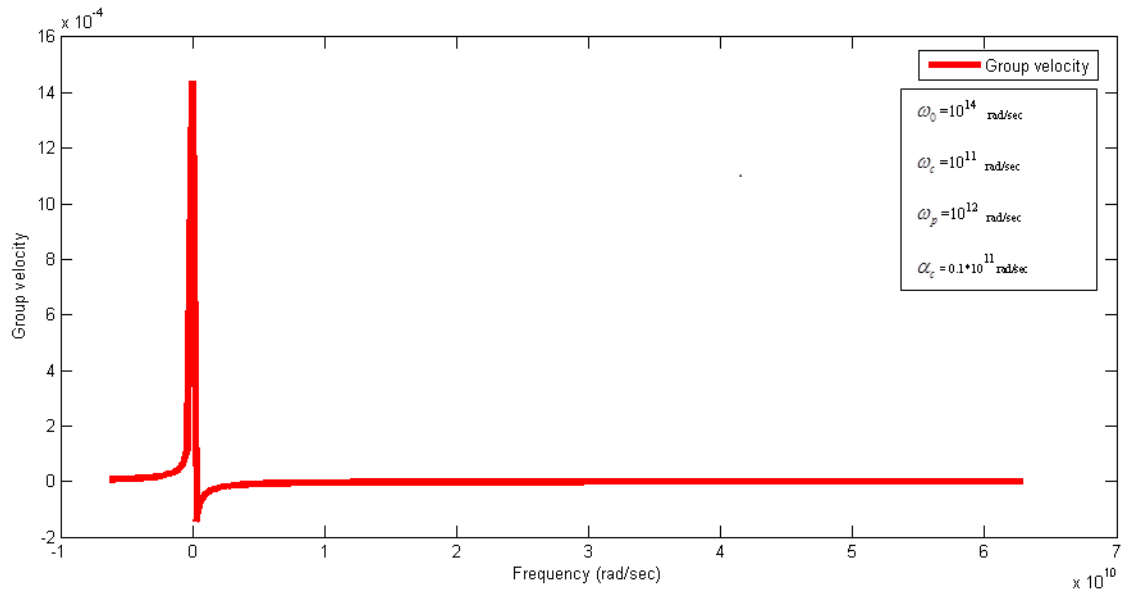

Figure 2. The Group velocity.

The group velocity again transition from positive to negative around the resonance. It is clear from the plot that the resonant frequency is approximately 2.52841×10^8 rad/s.

3.1 Note on direct comparison between $\tilde{v}_p$ and $\tilde{v_g}$

For the purpose of comparing the phase and group velocities for a given set of material constants across a range of frequencies, we discuss next the implications of the graphs in Figs.1 and 2. First, it must be noted that the graphs shown here represent the behavior of a material with second-order dispersion based on practical dispersive models. The resulting coefficients are thereafter matched to the derived solutions obtained from the spectral analysis carried out for the second-order dispersive system. Thus, the characteristics seen here may be considered somewhat closer to actual physical realizeability of such a system. We further note that the carrier frequency in the simulated graphs has been chosen to be about 10^{14} r/s, which is in the optical domain; on the other hand, the model resonance and the polarization and magnetization frequencies have been chosen to be around 10^{11} r/s and 10^{12} r/s respectively, The latter frequencies are clearly two to three orders of magnitude lower than the optical range. However, these frequencies physically represent sidebands (i.e., deviations Ω around the optical carrier) and are therefore expected to be in the higher RF to sub-mm wavelength range. From Figs.1 and 2, we observe that the sideband resonance for the phase velocity is around 10^{10} r/s, while that for the group velocity is around 2.5×10^8 r/s, indicating about a two-order-of-magnitude difference between these resonances. The significant result emerging from Figs.1 and 2 is related to the sign changes between $\tilde{v}_p$ and $\tilde{v}_g$. We observe that $\tilde{v}_p$ transitions from negative to positive around the resonance, while $\tilde{v}_g$ switches from positive to negative around its resonance. Thus, in the frequency range to the right of the $\tilde{v}_p$ resonance (i.e., higher than about 10^{10} r/s) indicates a positive phase velocity and a negative group velocity. Thus in this frequency range, the phase and group velocities are in opposition, and the material is likely in the negative index domain. Likewise, in the frequency range from 0 to 2.5×10^8 r/s, $\tilde{v}_p$ is negative, while $\tilde{v}_g$ is positive, and hence this range also may represent negative index behavior.

3.2 Estimation of negative index in the velocity counter-propagation regime

Noting that $n_{p3} \triangleq 1/v_{p3N}$, and $n_{g3} \triangleq 1/v_{g3N}$, we may straightforwardly plot the phase and group indices for the second-order dispersive system. These are shown in Figs.3 and 4. We observe that for the given value of the parameter $\beta \triangleq \frac{\omega_p}{\omega_c} = 10$ (for the simulations here), each of the indices experiences negative values (at frequencies below 10^{10} r/s for n_{p3}, and above 2.5×10^8 r/s for n_{g3} . However, the standard definition of negative index behavior indicates that velocity opposition only exists in the ranges as discussed in the previous section.

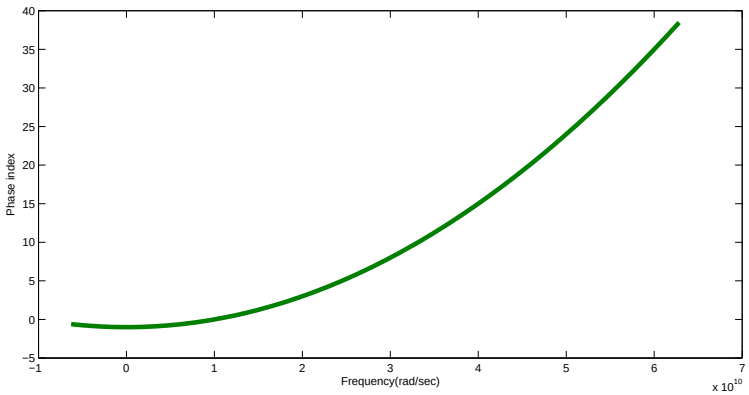

Figure 3. The phase index.

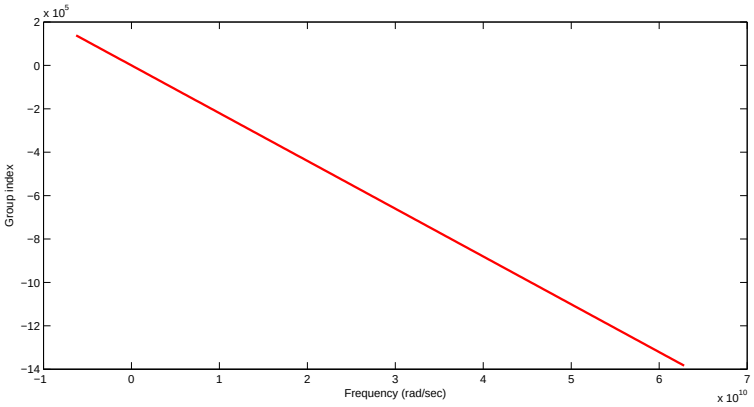

Figure 4. The group index.

4. CONCLUDING REMARKS

In this paper, we have discussed the phase and group velocities arising from a second-order material dispersion (up to Ω^2) in the presence of chirality. It is found that once again negative index may be realized under second-order conditions, specifically assuming practical dispersive models (such as Lorentz and Condon). It is demonstrated that there are measurable ranges of frequency where the phase and group velocities are in opposition for identical material properties. It is also observed that the velocities may co-propagate in regions where the phase and group indices may be negative together or individually; yet, based on the definition of negative behavior, the material is not in the negative index domain in such a frequency range. Further work will involve examining the phase and group indices in greater detail for other parametric and frequency conditions, and thereby assess the potential for negative index behavior in second-order dispersive systems. The results will also need to be compared with the first-order cases.

REFERENCES

[1] M. R. Chatterjee and T. A. Algadey, "Investigation of negative index in dispersive chiral materials via contra-propagating velocities under second-order dispersion GVD," *Proc. SPIE* **8837**, p. 88370W, 2013.

[2] P. P. Banerjee and M. R. Chatterjee, "Negative index in the presence of chirality and material dispersion," *J. Opt. Soc. Am. B* **26**, pp. 194–202, 2009.

[3] P. P. Banerjee and M. R. Chatterjee, "Consideration of dispersion and group velocity dispersion in the determination of velocities of electromagnetic propagation," *Proc. SPIE* **7797**, p. 779706, 2010.

[4] P. G. Zablocky and N. Engheta, "Transients in chiral media with single-resonance dispersion," *J. Opt. Soc. Am. B* **10**, pp. 740–753, 1993.

[5] J. B. Pendry, "Negative refraction," *Contemporary Physics.* **45**, pp. 191–202, 2004.

[6] V. G. Veselago, "Electrodaynamic of substances with simultaneously value of permativity and permability," *Sov. Phys. USP* **92**, pp. 517–526.

[7] P. P. Banerjee, R. Aylo, and G. Nehmetallah, "Baseband and envelope propagation in media modeled by a class of complex dispersion relations," *J. Opt. Soc. Am. B* **25**, pp. 990–994, 2008.